

^{29}Na : Defining the edge of the Island of Inversion for $Z = 11$

Vandana Tripathi¹, S.L. Tabor¹, P.F. Mantica^{2,3}, C.R. Hoffman¹, M. Wiedeking¹, A.D. Davies^{2,4}, S.N. Liddick^{2,3}, W.F. Mueller², T. Otsuka^{5,6}, A. Stolz², B.E. Tomlin^{2,3}, Y. Utsuno⁷, A. Volya¹

¹Department of Physics, Florida State University, Tallahassee, Florida 32306, USA

²National Superconducting Cyclotron Laboratory, Michigan State University, East Lansing, Michigan 48824, USA

³Department of Chemistry, Michigan State University, East Lansing, Michigan 48824, USA

⁴Department of Physics and Astronomy, Michigan State University, East Lansing, Michigan 48824, USA

⁵Dept. of Physics and Center for Nuclear Study, University of Tokyo, Hongo, Tokyo 113-0033, Japan

⁶RIKEN, Hirosawa, Wako-shi, Saitama 351-0198, Japan

⁷Japan Atomic Energy Research Institute, Tokai, Ibaraki 319-1195, Japan

(Dated: November 7, 2018)

The low-energy level structure of the exotic Na isotopes $^{28,29}\text{Na}$ has been investigated through β -delayed γ spectroscopy. The $N = 20$ isotones for $Z = 10 - 12$ are considered to belong to the “island of inversion” where intruder configurations dominate the ground state wave function. However, it is an open question as to where and how the transition from normal to intruder-dominated configurations happens in an isotopic chain. The present work, which presents the first detailed spectroscopy of $^{28,29}\text{Na}$, clearly demonstrates that such a transition in the Na isotopes occurs between ^{28}Na ($N = 17$) and ^{29}Na ($N = 18$), supporting the smaller $N = 20$ shell gap in neutron rich sd shell nuclei. The evidence for inverted shell structure is found in β decay branching ratios, intruder dominated spectroscopy of low-lying states and shell model analysis.

PACS numbers: 23.40.-s, 23.20.Lv, 21.60.Cs, 27.30.+t

Shell structure is one of the most fundamental properties of atomic nuclei that emphasizes the mean-field nature of nucleon dynamics. The spherical shells characterize the most stable configurations, the magic nuclei. However, from the pioneering studies of Thibault *et al.*, [1], it became apparent that the magic numbers may not be global and the $N = 20$ magic number may disappear in neutron-rich nuclei around $Z = 11$. The anomalously large binding energies for Na isotopes near $N = 20$ [1], the observation of low-lying first excited states with large $B(E2)$ transition probabilities to their ground states in ^{32}Mg [2, 3, 4], $^{28,30}\text{Ne}$ [3, 5], and ^{31}Na [6] and the measurements of large quadrupole moments in neutron-rich Na isotopes [7] are clear experimental signatures of this effect. The cause for this unexpected behavior, or “inversion” as it is called [8, 9], is due to the competition between the *normal* and *intruder* configurations (excitations across the $N = 20$ shell gap) with the intruder configurations becoming energetically favored. This emphasizes the phase transition from nucleon motion in the mean field to dynamics dominated by the residual nucleon-nucleon interactions.

For stable nuclei, the $N = 20$ shell gap separating the sd and fp shells is about 6 MeV, making it energetically costly for nucleons to occupy the fp orbitals. The “inversion” observed in neutron rich nuclei is related to the varying gap between the $d_{3/2}$ and $f_{7/2}$ orbitals which occurs due to the strong attractive interaction between the neutrons and protons occupying the spin-orbit coupling partners ($j_>$ and $j_<$) [10]. In exotic nuclei, due to the neutron-proton unbalance, the $j_<$ orbit is located rather high, reducing the gap with the higher shell. This reduced shell gap (~ 3 MeV) in the presence of residual

nucleon-nucleon interactions is not enough to sustain a shell structure. The transition from the normal to an intruder ground state depends primarily on the competition between shell structure and many body correlation effects due to residual interactions, which is a sensitive function of neutron number [11]. The open shell nuclei with $N < 20$ are very sensitive to the shell gap, as the gain in correlation energy for the intruder is not as large as for closed shell nuclei. The presence of intruder configurations at low excitation energy in transitional nuclei would be a signature of a small $N = 20$ shell gap. Recently, large scale Monte Carlo Shell Model (MCSM) calculations by Utsuno *et al.*, [12, 13] showed the intricate relation between the melting of shell structure and stability of exotic nuclei. The transition to an inverted state relates to the general question of phase changes in small systems, which unlike sharp changes in the thermodynamic limit exhibit gradual transitions accompanied by regions dominated by large fluctuations; furthermore particle number becomes of central importance.

In the present work we address this issue by approaching the $N = 20$ boundary along the Na isotopes. We have performed detailed β^- delayed γ -spectroscopy measurements of $^{28,29}\text{Na}$ ($N = 17, 18$) to investigate the transition from normal-dominant to intruder-dominant states in the chain of Na isotopes and its connection with the predicted small $N = 20$ shell gap for these neutron rich nuclei. Prior to the present work, very limited experimental information on excited states in these nuclei was available [15]. The level structures obtained from the present study clearly demonstrate the dominance of excitations across the $N = 20$ shell at low energies for ^{29}Na but a nearly pure sd shell configuration for ^{28}Na . This

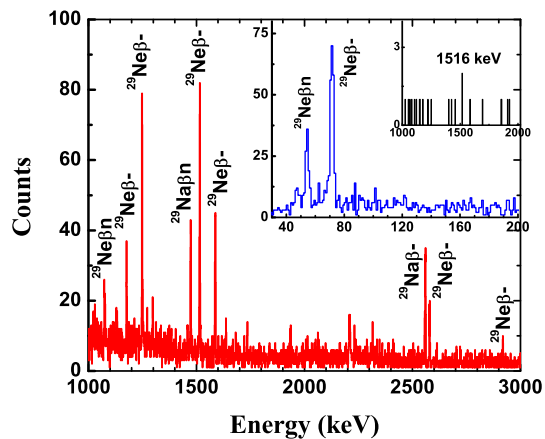


FIG. 1: (Color online) β^- delayed γ -ray spectrum in the range 1.0 - 3.0 MeV and 0 - 200 keV for events coming within the first 100 ms after a ^{29}Ne implant. γ -rays from ^{29}Ne β^- , β -n decay and ^{29}Na - β^- , β -n decay are indicated. The inset shows the β - γ - γ coincidences gated by 72 keV transition.

defines the extreme edge for the regime of intruder domination in Na isotopes, below which the intruder configurations cannot compete with normal configuration at small excitation.

Earlier comparisons of the experimental masses of the Na isotopes to shell model results within the sd shell (USD)[14] suggest that the “inversion” occurs sharply at $N = 20$. However comparison of the electric and magnetic moments of the Na isotopes [7] indicates a more gradual change; for the $N = 19, 20$ isotopes, the moments cannot be reproduced by the USD model, while the measured quadrupole moment of ^{29}Na ($N = 18$) is 30% larger than predicted by the USD model, and could be explained by considering $\sim 42\%$ mixing of intruder configurations in the ground state of ^{29}Na [11]. The spectrum of excited states provides another sensitive tool to probe the shell gap as well as the mixing between normal and intruder configurations. In particular, the relatively small $d_{3/2} - f_{7/2}$ shell gap estimated at about 3.3 MeV in recent calculations [11] for ^{29}Na can be tested by examining the low-energy excited states.

The parent nuclei, $^{28,29}\text{Ne}$, were produced by fragmentation of a 140 MeV/nucleon $^{48}\text{Ca}^{20+}$ beam in a 733 mg/cm² Be target located at the object position of the fragment separator, A1900, at the National Superconducting Cyclotron Laboratory (NSCL) at Michigan State University. A 300 mg/cm² wedge-shaped Al degrader was used at the intermediate image of the A1900 to disperse the fragments according to their M/Z ratios. The transport of $^{28,29}\text{Ne}$ ions was optimized in two settings of the A1900 magnetic fields: 4.52 Tm and 4.39 Tm with momentum acceptance of 1% for ^{28}Ne and 4.69 Tm and 4.56 Tm with momentum acceptance of 2% for ^{29}Ne . A “cocktail” secondary beam was obtained in both cases.

The yield of ^{29}Ne was ≈ 0.14 particles/s/pnA. The fully stripped fragments were implanted in a double sided Si micro-strip detector (DSSD), part of the Beta Counting System (BCS) [16] at NSCL. A 10 mm thick Al degrader was placed before the DSSD to ensure complete implantation within the DSSD. Fragments were unambiguously identified by a combination of multiple energy loss signals and time of flight. Each recorded event was tagged with an absolute time stamp generated by a free-running clock (30.5 μs repetition). Fragment- β correlations were established in software, a low-energy β event was correlated to a high-energy implant event in a same or adjacent pixels of the DSSD. Light particles were vetoed by a scintillator at the end of BCS, increasing the fragment- β correlation efficiency. The differences between the absolute time stamps of the correlated β and implant events were histogrammed to generate a decay curve. To suppress background, implants were rejected if they were not followed by a β event within a specified time period in the same (or neighboring) pixel or if a second implantation occurred before a β decay. A 100 ms time period was chosen for $^{28,29}\text{Ne}$ decay analysis. The β -delayed γ rays were detected using 12 detectors of the SEGmented Germanium Array (SeGA) [17] arranged around the BCS. The Ge detectors were energy and efficiency calibrated using standard calibrated sources.

The large Q_β window (>10 MeV) for neutron rich nuclei and small neutron separation energies (~ 4 MeV) in daughter nuclei allow for the population of many excited bound and neutron-unbound states after β^- decay. The β -delayed one and two neutron emission probabilities, P_n and P_{2n} , for $^{28,29}\text{Ne}$, have been extracted from the γ activities of the grand-daughter nuclei. The values obtained for ^{29}Ne are $29 \pm 7\%$ and $4 \pm 1\%$ respectively. P_n agrees well with the previous value of $27 \pm 9\%$ obtained by β -neutron coincidences [15], whereas no previous measurement of P_{2n} is reported. For ^{28}Ne β -decay, P_n and P_{2n} are $12 \pm 1\%$ and $3 \pm 1\%$ respectively. The half lives for the β -decay of $^{28,29}\text{Ne}$, extracted from a fitting of the decay curves, incorporating these neutron decay branches are 18.4 ± 0.5 ms and 13.8 ± 0.5 ms respectively, in agreement with reported values [18].

The energy spectra of β -delayed γ rays emitted within 100 ms (~ 5 half lives) of the arrival of an implant were generated for ^{28}Ne and ^{29}Ne . Parts of the spectrum for ^{29}Ne decay are shown in Fig. 1, where transitions associated with the β^- decay of ^{29}Ne are identified. Decay curves generated in coincidence with these γ lines yielded consistent half lives, justifying their placement in the level scheme of ^{29}Na , shown in Fig 2. The observation of pairs of lines, 1177 keV ($5\% \pm 1\%$) - 1249 keV ($12\% \pm 1\%$) and 1516 keV ($16\% \pm 2\%$) - 1588 keV ($11\% \pm 2\%$) differing by 72 keV and the observation of the 72 keV ($54\% \pm 9\%$) transition itself, confirms the first three excited states. The placement of the 1588 keV level is supported by the observed coincidence between the 72

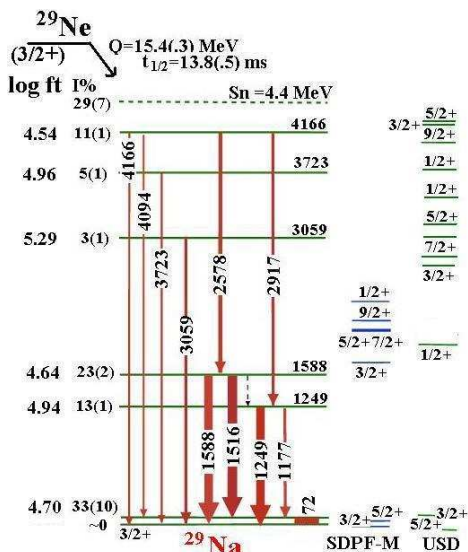


FIG. 2: (Color online) Proposed level scheme for ^{29}Na populated following the β -decay of ^{29}Ne . The absolute β -decay branching to each level per 100 decay is indicated along with the calculated $\log ft$ values. Shown on the right are shell model calculation with the USD and SDPF-M interactions.

keV and 1516 keV transitions (inset of Fig. 1). The other strong γ -rays, 2578 keV ($5\% \pm 1\%$) and 2917 keV ($3.5\% \pm 0.5\%$) depopulate the 4166 keV level. For ^{28}Ne decay, $\beta\gamma\gamma$ coincidences were the main guidelines in generating the level scheme. Coincidences for the 55 keV with 1076 keV, 2063 keV and 2659 keV transitions can be seen in Fig. 3, suggesting 4 levels at excitation energies of 55 keV, 1131 keV, 2118 keV and 2714 keV. The position of the 2714 keV state is corroborated by the 1583 keV - 1076 keV coincidences, while the 863 keV - 1255 keV cascade generates a level at 1255 keV. The γ - γ coincidences and energy and intensity sums allowed us to establish the detailed level scheme for ^{28}Na , shown in Fig. 4. The absolute intensities for β decay were calculated using the measured SeGA efficiency and the total number of $^{28,29}\text{Ne}$ decay events obtained from the decay curves. The $\log ft$ values were calculated from these β decay intensities (ignoring the weak unobserved transitions) according to Ref. [19].

A comparison of the level schemes for $^{28,29}\text{Na}$ from the current work with shell model calculations brings out interesting differences. Clearly the level structure for ^{29}Na (Fig. 2) is in stark disagreement with the USD predictions [14]. Apart from the ground state doublet (the order of which is reversed), the correspondence between the shell model predictions is not obvious. The experimental levels at 1249 keV and 1588 keV have large β^- decay branches, implying spin assignments of $1/2^+$, $3/2^+$ or $5/2^+$ (J^π of ^{29}Ne ground state is calculated to be $3/2^+$); however the USD calculations predict only one

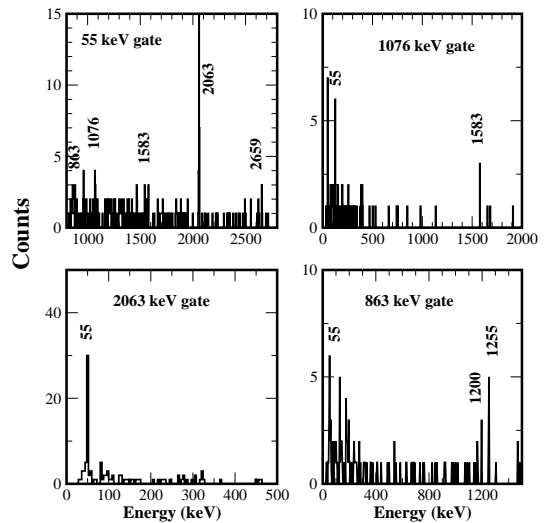


FIG. 3: The fragment- β - γ - γ coincidences for ^{28}Ne decay.

state ($1/2^+$) in this spin range below 2.8 MeV which has a small predicted β^- decay branch [20]. Also, within the USD shell model the almost degenerate states of the ground state doublet are expected to be equally populated via Gamow-Teller β^- decay transition, this contradicts observation. Allowing for excitations beyond the sd shell, the MCSM calculation with SDPF-M interaction [11], predicts the correct ground state spin of ^{29}Na ($3/2^+$ [21]). Four more states within the spin range, $1/2^+$ - $5/2^+$ are predicted below 2.5 MeV all with large probability of $2p2h$ excitations. The large β -decay branch to the 72 keV level makes it a likely candidate for the $5/2^+$ state predicted as a member of the ground state doublet. The $3/2^+$ (65% of $2p2h$ contribution), $5/2^+$ (78% of $2p2h$ contribution) are good candidates for the 1249 keV and 1588 keV experimental levels. The better agreement seen between the experimental results and the MCSM calculations suggests that fp intruder configurations play an important role in the low-energy level structure of $N = 18$ ^{29}Na . The present results also support a $3/2^+$ assignment to the ground state of ^{29}Ne , with strong $2p2h$ intruder mixing.

For ^{28}Na , the MCSM calculations predict low energy excited states which have almost pure $0p0h$ configurations in reasonable agreement with the USD calculations. Here intruder ($2p2h$) states involve the neutron excitation from the $1s_{1/2}$ orbital, at a higher energy cost. The correspondence between the experimental level structure of ^{28}Na and the calculations is quite good as demonstrated in Fig. 4. The ground state of ^{28}Na was previously assigned 1^+ [21], and the observation of a large β^- decay branch confirms the 1^+ assignment. The USD as well as MCSM calculations predict a 2^+ ground state and a 1^+ state with excitation energy less than 100 keV. It appears this doublet is reversed in nature and the ob-

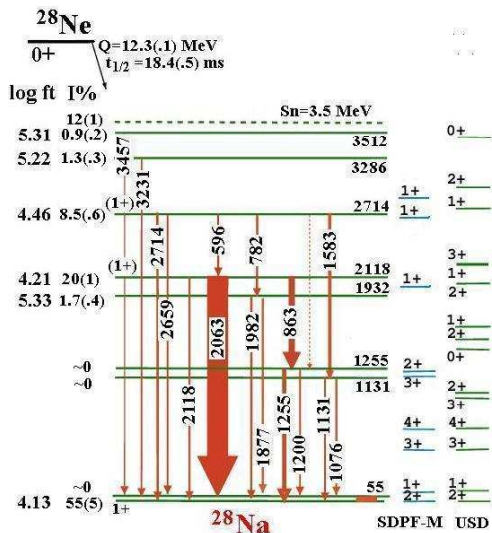


FIG. 4: (Color online) Proposed level scheme for ^{28}Na populated following the β^- decay of ^{28}Ne .

served 55 keV first excited state is almost certainly the predicted 2^+ level. Strong β^- decay branches from ^{28}Ne (0^+ ground state) have been observed to levels at 2118 keV and 2714 keV in the present work. These are likely the 1^+ states in good agreement with the MCSM calculations, though the USD shell model predicts their energies a bit lower. The shell model (USD) predicts $\approx 75\%$ of the total Gamow-Teller strength to go to the ground state and the first excited 1^+ state [20] in close agreement with the experimentally calculated $\log ft$ values. The 1255 keV state with negligible direct feeding most likely corresponds to the 1240(11) keV state seen by B.V. Pritychenko *et al.*, who assigned a spin of $J = 2$ [22]. Thus, there are candidates with closeby energies and $\log ft$ values in the USD shell model calculations, for the experimentally observed states, suggesting that ^{28}Na can be described rather well with pure sd shell configurations without invoking mixing of intruder configurations.

The presence of states at low excitation energy which have dominant $2p2h$ configuration in ^{29}Na points to the small $N = 20$ shell gap allowing for such intruder states. As suggested by Otsuka *et al.*, [10], the $N = 20$ shell gap evolves as a function of Z , being the smallest for O. Study of the level schemes for $^{25-28}\text{Ne}$ [3, 23] suggested that in the Ne isotopes, interference of intruders already starts at $N = 17$ and the neutron fp shell has to be included in the valence space in order to reproduce the data. However, the $N = 18$, ^{30}Mg [24] shows better agreement with the shell model predictions including only the sd shell. For the case of neutron rich Na isotopes, we find that ^{28}Na behaves nearly “normally”, as discussed above, but the $N = 18$ isotope, ^{29}Na , shows clear signatures of the influence of intruder configurations in its low energy level structure. Thus it is obvious that the intruder config-

uration mixing becomes important at $N = 17, 18, 19$ as we traverse from Ne to Mg via Na. This is a direct experimental signature of the evolution of the underlying $N = 20$ shell gap as a function of Z .

In summary, a study of the β^- decay of neutron-rich $^{28,29}\text{Ne}$ is reported. The low-energy level structure for the $N = 17, 18$ isotopes of Na have been established for the first time. Comparison of the level schemes and β^- branching ratios with theoretical shell model predictions, shows the influence of intruder configurations in the low-energy level structure of ^{29}Na , but not in ^{28}Na . For the Na isotopic chain, this is the first attempt to delineate the transition from the normal to intruder domination as seen in the low-energy level structure. The presence of states at low energy in ^{29}Na with dominant intruder configuration is a signature of the smaller shell gap compared to that of stable nuclei.

This work was supported by the NSF grants PHY-01-39950 and PHY-01-10253 and DoE grant DE-FG02-92ER40750. The authors thank the NSCL operations staff for the smooth conduct of the experiment.

-
- [1] C. Thibault *et al.*, Phys. Rev. C **12**, 644 (1975).
 - [2] T. Motobayashi *et al.*, Phys. Lett. B **346**, 9 (1995).
 - [3] B. V. Pritychenko *et al.*, Phys. Lett. B **461**, 322 (1999).
 - [4] V. Chiste *et al.*, Phys. Lett. B **514**, 233 (2001).
 - [5] Y. Yanagisawa *et al.*, Phys. Lett. B **566**, 84 (2003).
 - [6] B. V. Pritychenko *et al.*, Phys. Rev. C **63**, 011305(R) (2000).
 - [7] M. Keim, Proc. Conf. on Exotic Nuclei and Atomic masses, Bellaire, Michigan, June 23-27, 1998, p50 ; M. Keim *et al.*, Eur. Phys. J. A **8**, 31 (2000).
 - [8] E. K. Warburton, J. A. Pecker, and B. A. Brown, Phys. Rev. C **41**, 1147 (1990).
 - [9] E. Caurier *et al.*, Phys. Rev. C **58**, 2033 (1998).
 - [10] T. Otsuka *et al.*, Phys. Rev. Lett. **87**, 082502 (2001).
 - [11] Y. Utsuno *et al.*, Phys. Rev. C **70**, 044307 (2004).
 - [12] Y. Utsuno *et al.*, Phys. Rev. C **60**, 054315 (1999).
 - [13] Y. Utsuno *et al.*, Phys. Rev. C **64**, 011301(R) (2001).
 - [14] B. A. Brown and B. H. Wildenthal, Annu. Rev. Nucl. Part. Sci. **38**, 29 (1998).
 - [15] A. T. Reed *et al.*, Phys. Rev. C **60**, 024311 (1999).
 - [16] J. I. Prisciandaro *et al.*, Nucl. Instrum. Methods Phys. Res. A **505**, 140 (2003).
 - [17] W. F. Mueller *et al.*, Nucl. Instrum. Methods Phys. Res. A **466**, 492 (2003).
 - [18] M. Notoni *et al.*, Proc. Conf. on Exotic Nuclei and Atomic masses, Bellaire, Michigan, June 23-27, 1998, p359
 - [19] N. B. Gove and M. J. Martin, Nucl. Data Tables A **10**, 205 (1971).
 - [20] B. H. Wildenthal *et al.*, Phys. Rev. C **28**, 1343 (1983).
 - [21] G. Huber *et al.*, Phys. Rev. C **18**, 2342 (1978).
 - [22] B. V. Pritychenko *et al.*, Phys. Rev. C **66**, 024325 (2002).
 - [23] F. Azaiez, APH N.S. Heavy Ion Physics **12** (2000).
 - [24] P. Baumann *et al.*, Phys. Rev. C **39**, 626 (1989).